Automatic Modulation Classification of LFM and Polyphase-coded Radar Signals

Samer BAHER SAFA HANBALI, Radwan KASTANTIN

Dept. of Communication Engineering, Higher Institute of Applied Sciences and Technology, Damascus, Syria

Samer.Hanbali@hiast.edu.sy

Submitted December 4, 2016 / Accepted August 28, 2017

Abstract. *There are several techniques for detecting and classifying low probability of intercept radar signals such as Wigner distribution, Choi-Williams distribution and time-frequency rate distribution, but these distributions require high SNR. To overcome this problem, we propose a new technique for detecting and classifying linear frequency modulation signal and polyphase coded signals using optimum fractional Fourier transform at low SNR. The theoretical analysis and simulation experiments demonstrate the validity and efficiency of the proposed method.*

Keywords

LFM, polyphase coded signals, detection, automatic classification

1. Introduction

Electronic support measures (ESM) detect and classify low probability of intercept (LPI) radar signals, estimate their parameters and provide them to the jammer [1]. However, LPI radar signals have low power and large bandwidth that represent a great challenge to ESM [1].

ESM detection performance is inversely proportional to R^2 rather than to R^4 in the radar target detection equation. Therefore, the ESM can detect a radiating radar at distances far beyond those of the radar target detection capability. However, the radar's advantage is the use of matched filter that cannot be used by ESM receiver because it does not know the radar signal [2].

Several techniques depending on time-frequency distribution (TFD) were developed to identify and classify LPI radar signals. Examples of such technique are Wigner distribution (WD) [1] and Choi-Williams distribution (CWD) [3–5]. By using time-frequency techniques, one can obtain different time-frequency images for different radar signals. However, TFD has some shortcomings, for example, Wigner distribution images contain cross terms that make the measurement of the LPI signal parameters difficult. In order to attenuate these cross terms, smoothing operation (i.e. low-pass filtering) is needed, but this operation reduces time-frequency resolution [1]. In addition, WD requires huge calculations that makes it unsuitable for real time ESM systems. In CWD, the extraction of the modulation parameters is easier than it is in WD, because there is no strong cross terms in the time-frequency plane. The classification system is based on drawing a CWD image and extracting features from it. Time-frequency images are usually analyzed offline by a trained operator or by Bayesian neural networks to classify signals and extract their parameters accurately at high SNR (Signal to Noise Ratio) [5]. However, at lower SNR values, Choi-Williams kernel causes undesired horizontal and vertical lines in the CWD image [5]. In general, TFD performs well only at high SNR, but at low SNR, it is does not work [1]. Recently, a new method was introduced for detecting polyphase coded signals using time-frequency rate (TFR) distribution. However, it requires high SNR and there is no classifier for polyphase coded signals in this method [6].

All the above techniques of detection and classification of LFM (linear frequency modulation) signal and polyphase coded signals require a high SNR relatively. To overcome this problem, we propose to use fractional Fourier transform (FrFT). Compared with TFD, the FrFT is a linear operator and will not be influenced by cross-terms. This suggests that FrFT offers an advantage over using the TFD in practice. In addition, by using FrFT, the energy distribution of the LFM signal is more highly concentrated in the fractional domain [7]. Also, polyphase coded signals can be compressed by FrFT because these signals were developed by approximating LFM signal [2].

The paper is organized as follows. In Sec. 2, a short overview of used radar signals is introduced. In Sec. 3, pulse compression using FrFT is shown. In Sec. 4, the proposed detection and classification technique is presented. Finally, in Sec. 5, the performance of the proposed technique is demonstrated as a function of the SNR, and the obtained results are compared with the results of other techniques.

2. Overview of LFM Signal and Polyphase Coded Signals

LFM signal is commonly used in radar systems due to its high Doppler tolerance; the output of the matched filter remains approximately constant for Doppler shift up to $B/10$ [2], where B is the sweep bandwidth of LFM signal. The complex envelope of a LFM signal is given by:

$$x(t) = \mathrm{rect}(\frac{t}{T})\exp(\mathrm{j}\pi\mu t^2) \tag{1}$$

where rect is rectangular function, T is the pulse duration, and μ is the frequency modulation slope:

$$\mu = B/T. \tag{2}$$

In phase-coded signal, the long pulse of duration T is divided into N smaller sub-pulses called chips, each of width t_c:

$$t_c = T/N. \tag{3}$$

Each sub-pulse can be binary or polyphase modulated [2]. A polyphase-coded signal with unit energy is given by:

$$x(t) = \sum_{i=1}^{N}\mathrm{rect}\left(\frac{t-(i-1)t_c}{t_c}\right)\exp(\mathrm{j}\varphi_i)\cdot \tag{4}$$

Frank code and P1- through P4-code signals are examples of polyphase coded signals. Polyphase coded signals are commonly used in search and track radars due to their high Doppler tolerance and their ability to achieve low level time-sidelobes at the output of the matched filter. The phase element of the each polyphase code is given in Tab. 1 [2].

3. Pulse Compression using FrFT

The FrFT is a general form of the Fourier transform (FT) that transforms a function into an intermediate domain between time and frequency by rotating the time-frequency plane [8–9]. Compared with FT, the FrFT of optimal angle α_{opt} applied to a LFM signal, maximally concentrates the energy distribution of the signal in the fractional domain This illustrates the use of the FrFT for pulse compression of LFM signals [10].

Code	Phase
Frank	$\varphi_{i,j} = \frac{2\pi}{M}(i-1)(j-1)$ where $i, j = 1, 2, ..., M$, and $N = M^2$
P1	$\varphi_{i,j} = -\frac{\pi}{M}\left[M-(2j-1)\right]\left[(j-1)M+(i-1)\right]$ where $i, j = 1, 2, ..., M$, and $N = M^2$
P2	$\varphi_{i,j} = \left[\frac{\pi}{2}\left(\frac{M-1}{M}\right)-\frac{\pi}{M}(i-j)\right](M+1-2j)$ where $i, j = 1, 2, ..., M$, and $N = M^2$
P3	$\varphi_i = \left(\frac{\pi(i-1)^2}{N}\right)$ where $i = 1,..., N$.
P4	$\varphi_i = \left(\frac{\pi(i-1)^2}{N}\right)-\pi(i-1)$ where $i = 1,..., N$.

Tab. 1. The phase codes of polyphase signals.

The continuous FrFT of a signal $x(t)$ is given by [11]:

$$X_\alpha(u) = \int_{-\infty}^{\infty} x(t)K_\alpha(t,u)\mathrm{d}t \tag{5}$$

where $K_\alpha(t,u)$ is the transform kernel and when $\alpha \neq n\pi$ it equals [11]:

$$K_\alpha(t,u) = \sqrt{1-\mathrm{j}\cot\alpha}\exp(\mathrm{j}2\pi(\frac{t^2+u^2}{2})\cot\alpha - \mathrm{j}2\pi ut\csc\alpha) \tag{6}$$

where $\cot\alpha = 1/(\tan\alpha)$, and $\csc\alpha = 1/(\sin\alpha)$. Hence:

$$X_\alpha(u) = \int_{-\infty}^{\infty} x(t)\sqrt{1-\mathrm{j}\cot\alpha}\exp(\mathrm{j}2\pi(\frac{t^2+u^2}{2})\cot\alpha - \mathrm{j}2\pi ut\csc\alpha)dt. \tag{7}$$

If F_α denotes the operator corresponding to the FrFT of angle α, then the following properties hold [11]:

- $F_0 = I$: zero rotation gives the same input.
- $F_{\pi/2} = F$: rotation by $\pi/2$ gives Fourier transform.
- $F_\alpha(F_\beta) = F_{\alpha+\beta}$: successive rotations are additive. This means: $F_\alpha(F_{-\alpha}) = F_0 = I$.

Applying the FrFT to the LFM signal given by (1) gives:

$$X_\alpha(u) = A_\alpha\int_{-T/2}^{+T/2}\exp(\mathrm{j}\pi t^2(\mu+\cot\alpha) - \mathrm{j}2\pi ut\csc\alpha)\,\mathrm{d}t \tag{8}$$

where $A_\alpha = \sqrt{1-\mathrm{j}\cot\alpha}\exp(\mathrm{j}\pi u^2\cot\alpha)$. For arbitrary values of α, the integral in this equation involves an error function erf, which is a non-elementary function. But when:

$$\mu + \cot\alpha = 0. \tag{9}$$

A condition considered in [12] as being optimal and denoted by α_{opt}, then equation (8) reduces to the simple sinc function:

$$X_{\alpha_{opt}}(u) = A_\alpha T\frac{\sin(u\pi T\csc\alpha_{opt})}{(u\pi T\csc\alpha_{opt})}. \tag{10}$$

Usually, $\mu >> 1$, so equation (9) gives $\csc\alpha_{opt} = \mu$, and consequently, $|A_\alpha| = |\sqrt{1-\mathrm{j}\cot\alpha_{opt}}| = \sqrt{\mu}$. Hence [13]:

$$|X_{\alpha_{opt}}(u)| = \sqrt{BT}\frac{\sin(\pi Bu)}{(\pi Bu)}. \tag{11}$$

This is the same equation as that of the matched filter for LFM signal when $BT >> 1$. This means that the FrFT behaves like a matched filter for LFM signal [13].

Applying the FrFT to the polyphase coded signal given by (4) gives:

$$X_\alpha(u) = A_\alpha\int_0^T\sum_{i=1}^{N}\mathrm{rect}\left(\frac{t-(i-1)t_c}{t_c}\right)\exp(\mathrm{j}\varphi_i + \mathrm{j}\pi t^2\cot\alpha - \mathrm{j}2\pi ut\csc\alpha)\,\mathrm{d}t. \tag{12}$$

This solution involves an imaginary error function erfi (see Proof-1 at appendix) which can't be simplified analytically easily. Therefore, it can be evaluated numerically.

It is well known that the polyphase coded signal is a quantized form of the LFM signal [2]. Therefore, the optimal value of α is expected to be the same as that of the LFM signal, i. e. equation (9). The numerical search for α_{opt} confirms this hunch.

In [14] it was shown that FrFT may be obtained as a special case of the ambiguity function (AF) coordinate transformations. The AF of LFM signal has its energy concentrated along a diagonal ridge, but the AF of polyphase coded signal has two additional ridges on each side of the main ridge. Therefore, the main ridge energy of the P1, P2, and P4 codes is reduced by about 25% relative to the LFM signal, and the main ridge energy of the Frank and P3 codes are over 50% smaller than that of LFM signal [15], [16]. Consequently, the FRFT peak of LFM signal is greater than that of each of (P1, P2, P4) codes whose FRFT peak is greater than that of each of (Frank, P3) codes.

It was shown in [1] that LFM signal appears as a diagonal line in WD, whereas polyphase coded signal appears as several parallel lines separated by T in WD. In fact, the FRFT induces a simple rotation of the WD [11]. Consequently, the FRFT peaks of polyphase coded signal will be separated by $T_u = T\cos\alpha_{\mathrm{opt}}$. This equation is derived from the delay property of FrFT and confirmed by the numerical simulation. The pulse width of the detected signal is calculated as follows:

$$T = T_u / \cos\alpha_{\mathrm{opt}}. \tag{13}$$

Figure 1 shows the Matlab simulation results of the optimum FrFT of LFM signal and polyphase coded signals when $B = 5$ MHz and $T = 100$ µs. The following results can be shown:

- LFM signal has one global FRFT peak.
- (P1, P2, P4) signals have one global FRFT peak and several local peaks.
- (P3, Frank) signals have two global FRFT peaks separated by T_u and several local peaks.
- The global FRFT peak of LFM signal is greater than that of each of (P1, P2, and P4) codes whose global FRFT peak is greater than that of each of (Frank and P3) codes. Consequently, the detection performance of LFM signal is better than that of each of (P1, P2, P4) codes whose detection performance is better than that of each of (P3, Frank) codes.

It has been shown that the FrFT can compress LFM and polyphase coded signals. The SNR at the output of FrFT equals $SNR_{\mathrm{o}} = SNR_{\mathrm{i}} + G$, where SNR_{i} is the signal to noise ratio at the input of the FrFT, and $G = BT >> 1$ is the pulse compression gain, therefore FrFT can be used to detect the input signal at low SNR.

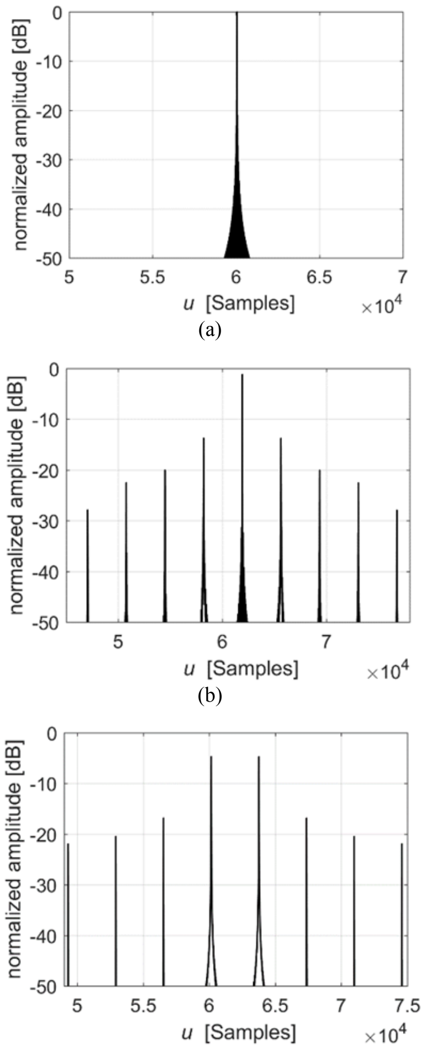

Fig. 1. Optimum FrFT of: (a) LFM, (b) (P1, P2, P4), (c) (Frank, P3).

In the discrete domain the optimum transform angle α_{opt} of the FrFT is given by [17], [7]:

$$\alpha_{\mathrm{opt}} = -\tan^{-1}\left(\frac{F_{\mathrm{s}}^2}{\mu.L}\right) \tag{14}$$

where L is the number of samples in the time received window, and F_{s} is the sampling frequency.

In practice, the optimal transform angle is not known in advance. Therefore, peak search is necessary to find the optimal transform angle with which the energy distribution of LFM signal concentrates well. However, this search is time consuming so the parameter searching problem can be solved by using the new strategy proposed in [18], which combines the principle of golden and the quasi-Newton iterative method, when it searches the signal FRFT peak, and then it takes advantage of the quasi-Newton iterative method to reduce the step size selection on the optimal transform order estimation accuracy, and achieves the same accuracy while reducing the computational search.

4. The Proposed Technique for Detection and Classification

In the case of intercept radar, the aim is to detect the parameters of the transmitted pulse such as duration and bandwidth. The block diagram of the proposed detection and classification technique is shown in Fig .2, where $r(t)$ is the baseband received signal that is composed of the sum of the radar signal $x(t)$, and a white Gaussian noise $n(t)$.

The process of the proposed technique is shown in Fig. 2, and it goes as follows:

1. Start computing FrFT and use a search method in order to tune the transform order α_{opt} that gives the maximum magnitude response of FrFT, the received radar signal is compressed using FrFT at α_{opt} as shown in Fig. 3.
2. The local peaks could be buried in noise at low SNR as shown in Fig. 3, therefore only the global FRFT peak could be detected by CA-CFAR (cell average constant false alarm rate).
3. The sample of each global FRFT peak and its adjacent samples (main lobe) are kept, and all other samples in the received window are put to zero to get the filtered signal in the optimal FrFT domain as shown in Fig. 4.
4. Measure T_u when there are two global FRFT peaks as shown in Fig. 4(c). In this case, the filtered signal is Frank code or P3 code. Otherwise, the filtered signal is LFM or (P1, P2, P4) code, then the bandwidth of this signal is estimated by returning it to the frequency domain using FrFT at the complementary value of α_{opt}, i.e. $\pi/2 - \alpha_{\text{opt}}$ as shown in Fig. 5. It is well known that the shape of LFM spectrum is rectangular, therefore its bandwidth is determined at –3 dB level, whereas the shape of P1, P2, P4 codes spectrum follows a sinc function, therefore its bandwidth is determined at –4 dB level. However, the detected signal is unknown, therefore both –3 dB bandwidth and –4 dB bandwidth of the filtered signal are determined.
5. The frequency modulation slope is calculated by using (14).
6. Calculate the parameters (B, T, t_c, N) of the detected signal using (2), (3), and (13).
7. Now, in order to classify the detected radar signal, some reference signals will be generated depending on the estimated parameters (B, T, t_c, N) of the previous step. If the received signal is classified in the first group (P3, Frank) because it has two global FRFT peaks, only P3 and Frank reference signals are generated, otherwise only LFM and (P1, P2, P4) reference signals are generated at –3 dB bandwidth and –4 dB bandwidth, respectively. Finally, the input signal is classified to the reference signal that has the highest cross-correlation with it.

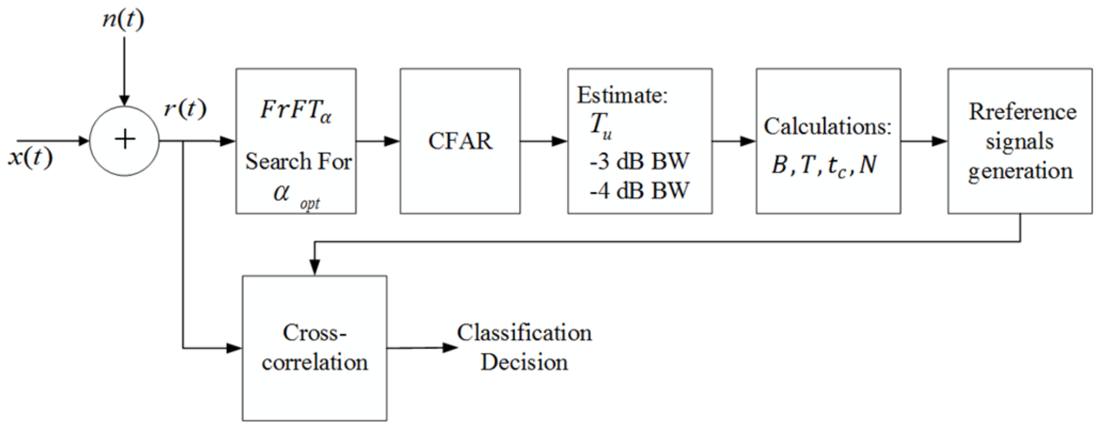

Fig. 2. The block diagram of the proposed detection and classification technique.

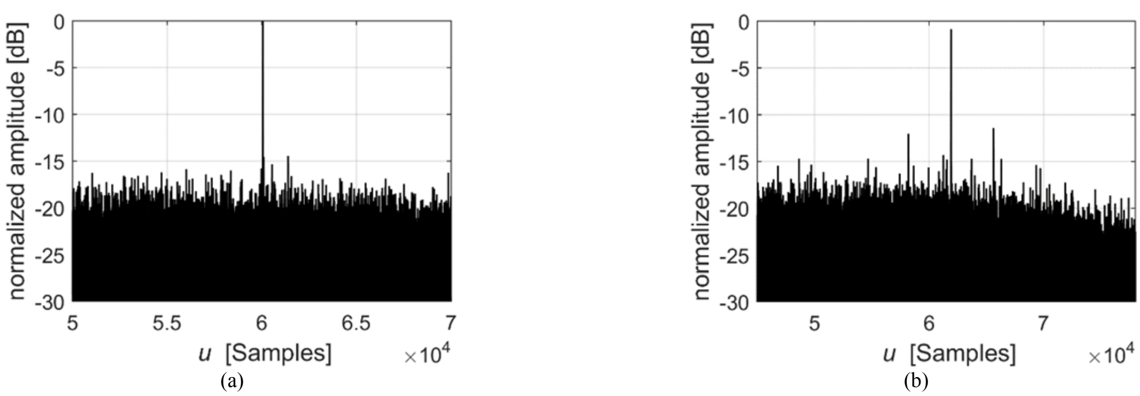

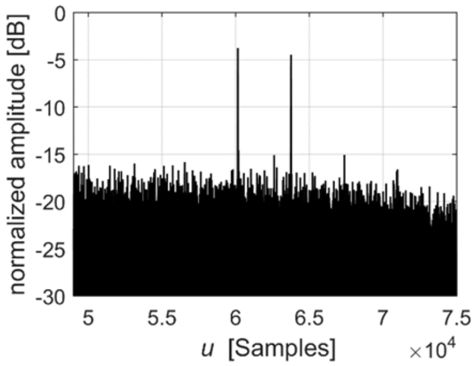

(c)

Fig. 3. Optimum FrFT in the presence of noise: (a) LFM, (b) (P1, P2, P4), (c) (Frank, P3).

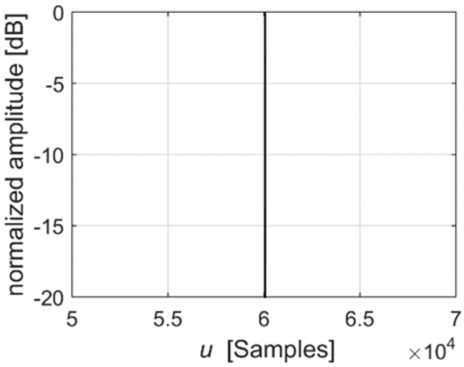

(a)

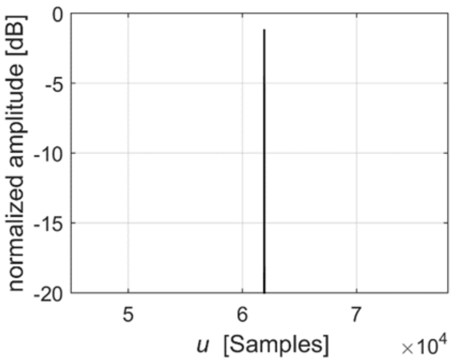

(b)

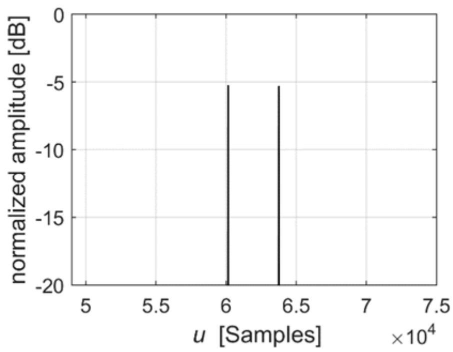

(c)

Fig. 4. Filtered signal in fractional domain: (a) LFM, (b) (P1, P2, P4), (c) (Frank, P3).

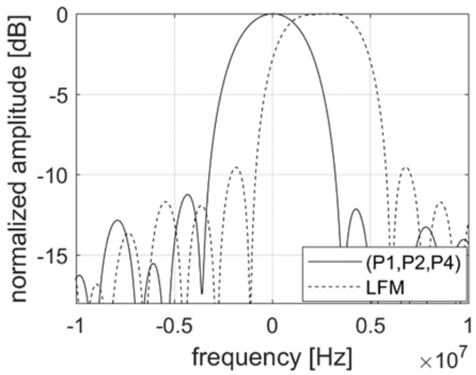

Fig. 5. The spectrum of the filtered signal.

The computation complexity of the proposed technique depends on the implementation of FrFT. The fast FrFT is approximated using algorithms based on the fast Fourier transform (FFT), and it was shown that the fast FrFT has a computational complexity $O(N\log N)$ [8], [9], which is suitable for practical application [17].

5. Simulation and Results

In order to evaluate the performance of the proposed technique, different LFM signals and polyphase coded signals are generated in the presence of additive noise and under different SNR values of the received signal $r(t)$. Then the Monte-Carlo simulation of 1000 trials for each SNR used to estimate the probability of detection P_d of each signal. Figure 6 shows the simulation results of P_d, as a function of SNR, for LFM signal and polyphase coded signals when $B = 5$ MHz, $T = 100$ µs.

The following results are shown in Fig. 6:

1. The FrFT is inferior to the matched filter by 3 dB in the case of LFM signal [19].
2. The CA-CFAR causes a loss of about 0.4 dB in SNR when the number of the reference cells equals 50 and the probability of false alarm $P_{fa} = 10^{-4}$ [20].
3. The proposed technique achieves high probability (about 90%) of successful detection under low SNR. In comparison with other works, the proposed technique works well at lower SNR than those based on time-frequency distributions and on time-frequency rate.
4. The detection performance of LFM signal is better than that of each of (P1, P2, and P4) codes whose detection performance is better than that of each of (Frank, P3) codes, because a higher FrFT peak leads to a better detection performance. Consequently, P3 coded signal could be preferable to be used in LPI radars, first because it has lower detection performance that makes it difficult to be intercepted by ESM, and second because it has high Doppler tolerance [2].

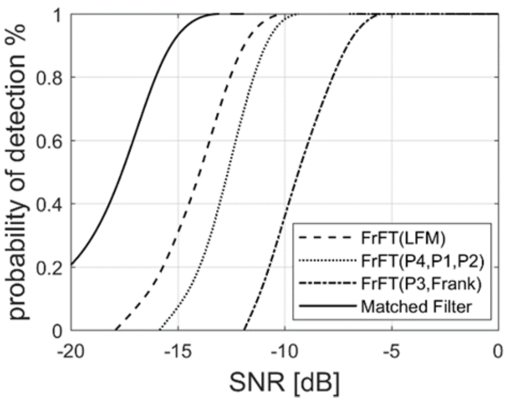

Fig. 6. Detection performance of LFM signal and polyphase codes when $B = 5$ MHz, $T = 100$ µs.

The cross-correlation is used for signals classification, which is only optimal in the case of the generated reference signal maintaining the original properties of the detected signal. In this case, the reference signals will be generated accurately, and the input signal is classified to the reference signal that has the highest cross-correlation with it. Figure 7 and 8 show the classification results of the detected signals (LFM, P1, P2, P4) and (P3, Frank) respectively.

Figure 7 shows that the classification performance of LFM signal is better than that of P1, P2, and P4 codes because these codes are a quantized form of the LFM signal [2], therefore a classification confusion between the LFM signal and (P1, P2, P4) codes occurs especially at low SNR. But as the SNR increases this confusion decreases.

Figure 8 shows that the classification performance of (P3, Frank) codes is similar to their detection performance shown in Fig. 6, because of the search for the two global FRFT peaks, as mentioned above in the proposed technique, is considered as a detection and as an initial classification simultaneously. Then, the input signal (P3, Frank) is classified accurately to the reference signal that has the highest cross-correlation with it. The proposed technique achieves high probability (about 90%) of successful classification under low SNR. In comparison with other works, the proposed technique works well at lower SNR than those based on time-frequency distributions and on time-frequency rate.

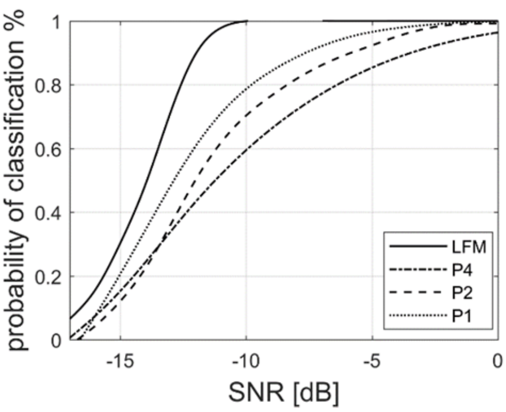

Fig. 7. Classification performance of LFM signal and (P1, P2, P4) codes when $B = 5$ MHz, $T = 100$ µs.

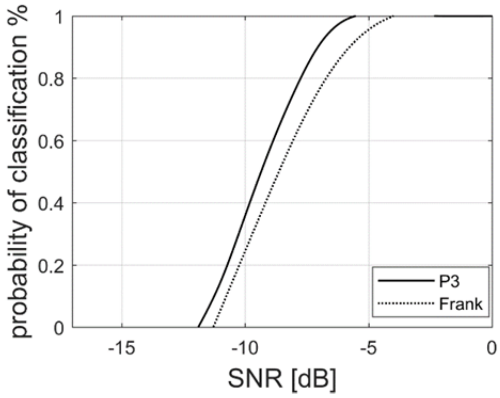

Fig. 8. Classification performance of (P3, Frank) codes when $B = 5$ MHz, $T = 100$ µs.

It has been shown that the proposed technique has two advantages over other methods, first because it works under low SNR where other methods do not work, and second because it classifies signals without using complicated neural networks like TFD methods.

6. Conclusion

In this paper, a new technique for detecting and classifying LFM signal and polyphase coded signals is proposed. This technique is based on the optimum fractional Fourier transform, and it requires few calculations so the ESM can estimate radar signal's parametric data in near real time. The performance of the proposed technique is demonstrated as a function of SNR using Monte-Carlo simulation. The simulation results show that the proposed technique has the advantages over other techniques because it has accurate detection and classification at low SNR.

Acknowledgement

The authors would like to thank Hatem Najdi for his helpful discussions and for reviewing the final version of this paper.

References

[1] PACE, P. E. *Detecting and Classifying Low Probability of Intercept Radar.* Artech House, 2009. ISBN: 978-1596932340

[2] SKOLIK, M. *Radar Handbook.* 3rd ed. McGraw-Hill, 2008. ISBN: 978-0071485470

[3] LUNDEN, J., TERHO, L., KOIVUNEN, V. Classifying pulse compression radar waveforms using time-frequency distributions. In *Proc. 39th Annual Conf. Information Sciences and Systems (CISS 2005)*. Baltimore (USA), 2005.

[4] LUNDEN, J., TERHO, L., KOIVUNEN, V. Waveform recognition in pulse compression radar systems. In *2005 IEEE Workshop on Machine Learning for Signal Processing.* Mystic (CT, USA), 2005, p. 271–276. DOI: 10.1109/MLSP.2005.1532912

[5] LUNDEN, J., KOIVUNEN, V. Automatic radar waveform recognition. *IEEE Journal of Selected Topics in Signal Processing*, 2007, vol. 1, no. 1, p. 124–136. DOI: 10.1109/JSTSP.2007.897055

[6] JIANG, L., LI, L., ZHAO, G. Q. Polyphase coded low probability of intercept signals detection and estimation using time-frequency rate distribution. *IET Signal Processing*, 2016, vol. 10, no. 1, p. 46–54. DOI: 10.1049/iet-spr.2014.0020

[7] ELGAMEL, S. A., CLEMENTE, C., SORAGHAN, J. J. Radar matched filtering using the fractional Fourier transform. In *Sensor Signal Processing for Defence (SSPD 2010)*. London (UK), 2010, 5 p. DOI: 10.1049/ic.2010.0242

[8] OZAKTAS, H. M., ARIKAN, O., KUTAY, M. A., BOZDAGT, G. Digital computation of the fractional Fourier transform. *IEEE Transactions on Signal Processing*, 1996, vol. 44, no. 9, p. 2141 to 2150. DOI: 10.1109/78.536672

[9] CANDAN, C., KUTAY, M. A., OZAKTAS, H. M. The discrete fractional Fourier transform. *IEEE Transactions on Signal Processing*, 2000, vol. 48, no. 5, p. 1329–1337. DOI: 10.1109/78.839980

[10] SUN, H. B., LIU, G. S., GU, H., et al. Application of the fractional Fourier transform to moving target detection in airborne SAR. *IEEE Transactions on Aerospace and Electronic Systems*, 2002, vol. 38, no. 4, p. 1416–1424. DOI: 10.1109/TAES.2002.1145767

[11] ALMEIDA, L. B. The fractional Fourier transform and time–frequency representations. *IEEE Transactions on Signal Processing,* 1994, vol. 42, no. 11, p. 3084–3091. DOI: 10.1109/78.330368

[12] CAPUS, C., BROWN, K. Short-time fractional Fourier methods for the time-frequency representation of chirp signals. *Journal of Acoustical Society of America*, 2003, vol. 113, no. 6, p. 3253 to 3263. DOI: 10.1121/1.1570434

[13] BAHER SAFA HANBALI, S., KASTANTIN, R. Fractional Fourier transform-based chirp radars for countering self-protection frequency-shifting jammers. *International Journal of Microwave and Wireless Technologies*. [Online] Cited April 3, 2017, 7 p. DOI: 10.1017/S1759078717000289

[14] DJUROVIĆ, I., STANKOVIĆ, L. Relationship between the ambiguity function coordinate transformations and the fractional Fourier transform. *Annals of Telecommunications*, 1998, vol. 53, no. 7, p. 316–319.

[15] JANKIRAMAN, M. *Design of Multi-Frequency CW Radars*. SciTech Publishing Inc., 2007. ISBN: 978-1891121562

[16] JENNISON, B. K. Detection of polyphase pulse compression waveforms using the radon-ambiguity transform. *IEEE Transactions on Aerospace and Electronic Systems*, 2003, vol. 39, no. 1, p. 335–343. DOI: 10.1109/TAES.2003.1188915

[17] COWELL, D. M., FREEAR, S. Separation of overlapping linear frequency modulated (LFM) signals using the fractional Fourier transform. *IEEE Transactions on Ultrasonics, Ferroelectrics, and Frequency Control*, 2010, vol. 57, no. 10, p. 2324–2333. DOI: 10.1109/TUFFC.2010.1693

[18] XIN, L., JIANG, Y. Y. Golden-section peak search in fractional Fourier domain. In *IEEE International Conference on Electric Information and Control Engineering (ICEICE).* Wuhan (China), 2011, p. 4230–4233. DOI: 10.1109/ICEICE.2011.5778100

[19] LIU, J. C., LIU, Z., WANG, X. S., et al. SNR analysis of LFM signal with Gaussian white noise in fractional Fourier transform domain. *Journal of Electronics and Information Technology*, 2007, vol. 29, no. 10, p. 2337–2340. (in Chinese) DOI: 10.3724/SP.J.1146.2006.00314

[20] RICHARDS, M. *Fundamentals of Radar Signal Processing.* 2nd ed., McGraw-Hill, 2014. ISBN: 978-0-07-179833-4

About the Authors...

Samer BAHER SAFA HANBALI received the B.Sc. degree in Electronic Engineering from Damascus University, Syria, in 2000, the M.Sc. degree from FH-Joanneum, Austria, in 2011, and the Ph.D. degree from the Higher Institute of Applied Sciences and Technology, Damascus, Syria, in July 2017. He works in the same institute, and his current research is focused on radar signal processing.

Radwan KASTANTIN received the B.Sc. degree in Electronic Engineering from Damascus University, Syria, in 1986, and the Ph.D. degree from ICP-INPG, France, in 1996. He is a professor of communication and signal processing at the Dept. of Communication Engineering in the Higher Institute of Applied Sciences and Technology, Damascus, Syria.

Appendix: Proof-1

The FrFT of polyphase coded signals equals:

$$X_\alpha(u)=\sqrt{1-\mathrm{j}\cot\alpha}\exp(\mathrm{j}\pi u^2\cot\alpha)\int_0^T\sum_{i=1}^N\mathrm{rect}(\frac{t-(i-1)t_\mathrm{c}}{t_\mathrm{c}})$$
$$\exp(\mathrm{j}\varphi_i+\mathrm{j}\pi t^2\cot\alpha-\mathrm{j}2\pi ut\csc\alpha)\,\mathrm{d}t. \tag{A.1}$$

Then:

$$X_\alpha(u)=\sqrt{1-\mathrm{j}\cot\alpha}\exp(\mathrm{j}\pi u^2\cot\alpha)\sum_{i=1}^N\exp(\mathrm{j}\varphi_i)$$
$$\int_{(i-1)t_\mathrm{c}}^{it_\mathrm{c}}\exp(\mathrm{j}\pi t^2\cot\alpha-\mathrm{j}2\pi ut\csc\alpha)\,\mathrm{d}t. \tag{A.2}$$

Let’s define the integral I

$$I=\int_{(i-1)t_\mathrm{c}}^{it_\mathrm{c}}\exp(\mathrm{j}(pt^2-qut))\,\mathrm{d}t \tag{A.3}$$

where: $p=\pi\cot\alpha$, $q=2\pi\csc\alpha$, equation (A.3) can be rewritten:

$$I=\int_{(i-1)t_\mathrm{c}}^{it_\mathrm{c}}\exp(\mathrm{j}((\sqrt{p}t-\frac{qu}{2\sqrt{p}})^2-\frac{q^2u^2}{4p}))\,\mathrm{d}t$$
$$=\exp(-\mathrm{j}\frac{q^2u^2}{4p})\int_{(i-1)t_\mathrm{c}}^{it_\mathrm{c}}\exp(\mathrm{j}(\sqrt{p}t-\frac{qu}{2\sqrt{p}})^2)\,\mathrm{d}t. \tag{A.4}$$

Let’s define z: $$z=\sqrt{p}t-\frac{qu}{2\sqrt{p}}. \tag{A.5}$$

Hence: $$\mathrm{d}t=\frac{\mathrm{d}z}{\sqrt{p}}. \tag{A.6}$$

By substitution (A.5) and (A.6) in (A.4) then:

$$I=\frac{1}{\sqrt{p}}\exp(-\mathrm{j}\frac{q^2u^2}{4p})\int_{L_1}^{L_2}\exp(\mathrm{j}z^2)\mathrm{d}z \tag{A.7}$$

where: $L_1=\sqrt{p}(i-1)t_\mathrm{c}-\frac{qu}{2\sqrt{p}}$, and $L_2=\sqrt{p}it_\mathrm{c}-\frac{qu}{2\sqrt{p}}$.

By substitution the following expression in (A.4):

$$\int_{L_1}^{L_2} \exp(\mathrm{j}z^2)\,\mathrm{d}z = \frac{\sqrt{\pi}}{2\sqrt{\mathrm{j}}}\left[\mathrm{erfi}\left(\sqrt{\mathrm{j}}L_2\right) - \mathrm{erfi}\left(\sqrt{\mathrm{j}}L_1\right)\right] \quad (A.8)$$

where erfi is the imaginary error function. Hence:

$$I = \frac{\sqrt{\pi}}{2\sqrt{\mathrm{j}p}} \exp(-\mathrm{j}\frac{q^2u^2}{4p})[\mathrm{erfi}\left\{\sqrt{\mathrm{j}}\left(\sqrt{p}it_\mathrm{c} - \frac{qu}{2\sqrt{p}}\right)\right\} - \mathrm{erfi}\left\{\sqrt{\mathrm{j}}\left(\sqrt{p}(i-1)t_\mathrm{c} - \frac{qu}{2\sqrt{p}}\right)\right\}]. \quad (A.9)$$

By substitution (A.9) in (A.2):

$$X_\alpha(u) = \frac{\sqrt{\pi}\sqrt{1-\mathrm{j}p/\pi}}{2\sqrt{\mathrm{j}p}} \exp(\mathrm{j}(pu^2 - \frac{q^2u^2}{4p}))\sum_{i=1}^{N}\exp(\mathrm{j}\varphi_i)$$
$$\times[\mathrm{erfi}\{\sqrt{\mathrm{j}}(\sqrt{p}it_\mathrm{c} - \frac{qu}{2\sqrt{p}})\} - \mathrm{erfi}\{\sqrt{\mathrm{j}}(\sqrt{p}(i-1)t_\mathrm{c} - \frac{qu}{2\sqrt{p}})\}]. \quad (A.10)$$

Since analytic expression cannot be easily obtained, this equation was evaluated by numerical computation as mentioned before.